

Dynamics of stimulated emission in silicon nanocrystals

L. Dal Negro,^{a)} M. Cazzanelli, and L. Pavesi

INFN-Dipartimento di Fisica, Università di Trento, via Sommarive 14, I-38050 Povo (Trento), Italy

S. Ossicini

INFN-S,³ and Dipartimento di Scienze e Metodi dell'Ingegneria, Università di Modena e Reggio Emilia, via Allegrì 13, I-42100 Reggio Emilia, Italy

D. Pacifici, G. Franzò, and F. Priolo

INFN-Dipartimento di Fisica e Astronomia, Università di Catania, via S. Sofia 64, I-95123 Catania, Italy

F. Iacona

CNR-IMM, Sezione di Catania, I-95121 Catania, Italy

(Received 16 January 2003; accepted 23 April 2003)

Time-resolved luminescence measurements on silicon nanocrystal waveguides obtained by thermal annealing of plasma-enhanced chemical-vapor-deposited thin layers of silicon-rich oxide have revealed fast recombination dynamics related to population inversion which leads to net optical gain. Variable stripe length measurements performed on the fast emission signal have shown an exponential growth of the amplified spontaneous emission with net gain values of about 10 cm^{-1} . The fast emission component is strongly dependent on the pumping length for fixed excitation intensity. In addition, both the fast component intensity and its temporal decay revealed threshold behavior as a function of the incident pump intensity. © 2003 American Institute of Physics.

[DOI: 10.1063/1.1586779]

One of the main future challenges for silicon microphotonics consists in the demonstration of a laser action in silicon-based gain materials.^{1,2} Following the initial observations of optical gain in silicon nanocrystals (Si-nc) prepared by ion implantation,³ other works have recently demonstrated the presence of stimulated emission in Si-nc.^{4–6} As in other quantum dot-based systems,^{7,8} a severe competition with efficient nonradiative processes, mainly nonradiative Auger processes, is present in Si-nc yielding very fast dynamics in the optical gain.⁴ Although a clear understanding of the microscopic gain mechanism is still under debate, it has been suggested that interface radiative states associated with oxygen atoms can play a crucial role in determining the emission properties of the Si-nc systems.^{9,10} Here, we report on light amplification dynamic studies in Si-nc and discuss a possible gain model.

Si-nc samples were produced by high-temperature annealing of substoichiometric silicon oxide (SiO_x) thin films grown by plasma-enhanced chemical-vapor deposition on a quartz substrate. The structural and luminescence properties of these systems have been fully discussed elsewhere.¹¹ Here, we focus on a sample produced with a total silicon content of 42 at. % and annealed at 1250 °C for 1 h which yields closely packed Si ncs with a mean diameter of 1.7 nm and a size distribution 1.1 nm wide. Such a wide size distribution is reflected in a wide luminescence band (188 nm wide) peaked at 908 nm. The Si-nc-rich layer (250 nm thick) was embedded between two 100 nm thick amorphous SiO_2 layers to form an optical waveguide. Considering a refractive index of 1.82,¹¹ the optical confinement factor of the waveguide was estimated to be 74%.

This sample shows optical gain in continuous wave measurements.¹² To investigate the stimulated emission dynamics, time-resolved experiments were performed in the one-dimensional amplifier configuration (pumping through the surface and collection of the guided light from one edge of the sample). This method, also called the variable stripe length (VSL) method,¹³ measures the amplified spontaneous emission (ASE) as a function of the excitation length ℓ and allows measuring the stimulated emission build-up time as the signal photons propagate along the amplification axis. Although simple in principle, VSL techniques applied to Si ncs can present some experimental difficulties which have been fully discussed elsewhere.^{14,15} High fluence short optical pulses (6 ns, 10 Hz, and 355 nm) produced by the third harmonic of a Nd-YAG laser were used to excite the samples. A single grating spectrometer and a visible streak camera have been used to detect the time-resolved signal. Edge emission was collected by a 20× optical microscope objective with a numerical aperture of 0.3, which is larger than the output numerical aperture of the waveguide sample, allowing for constant collection efficiency over the whole pumping length.¹⁵ Special care has been used both to keep the fluence lower than the sample damage threshold and to avoid the collection of stray light of the pump laser pulses.¹²

When measurements are performed in the usual luminescence configuration (emission collected through the sample surface) and at low pumping fluence J_p , the luminescence decays are stretched exponentials with observation energy dependent lifetimes in the range of 10 to 50 μs .^{12,16} However, when the VSL configuration is used, a fast ns decay component shows up.⁴ Figure 1(a) shows the normalized edge emission intensity decay as a function of J_p for a long excitation length. At low J_p , a simple decay is observed with a slow rate slightly dependent on the fluencies, while at high J_p , a fast decay component emerges which is superimposed

^{a)}Present address: Materials Processing Center, Department of Materials Science and Eng., Massachusetts Institute of Technology; electronic mail: dalnegro@mit.edu

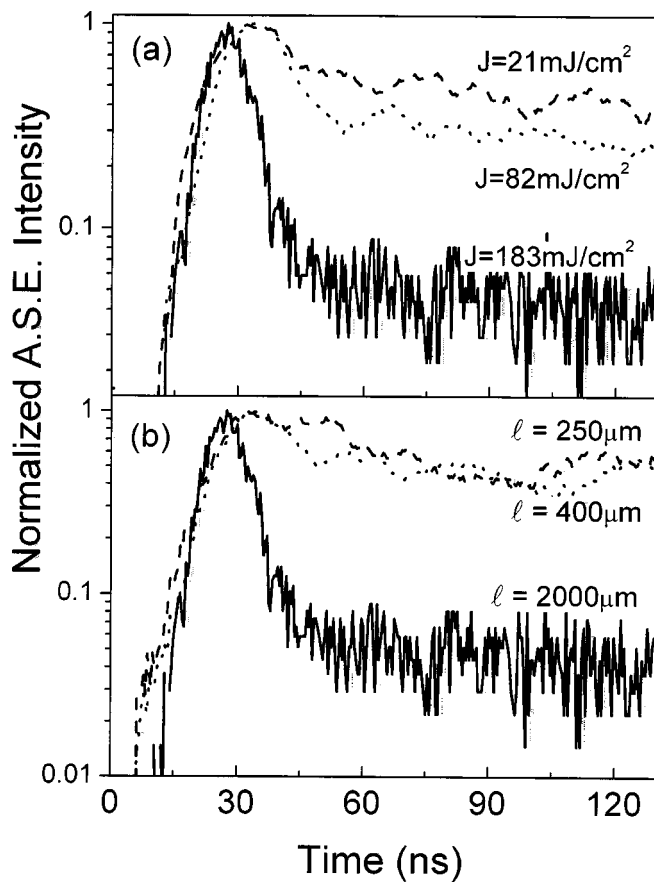


FIG. 1. (panel a) Normalized ASE at 760 nm measured in the VSL geometry with a fixed pumping length $\ell=2$ mm and at the different pumping fluences reported on the plots. (panel b) Normalized ASE at 760 nm measured in the VSL geometry with the various pumping length reported on the plots and for a fixed pumping fluence of 183 mJ/cm².

to the *slow* component. The fast component of the ASE signal has some very peculiar characteristics:

- (i) It disappears when either the excitation length ℓ is decreased at a fixed J_p [Fig. 1(b)] or when J_p is decreased for a fixed ℓ [Fig. 1(a)], i.e., it is not only related to the pump photon flux density (fluence) but also to the length of the one-dimensional amplifier. The fast component intensity also depends on the signal photon flux density all along the pumped region.
- (ii) Its peak intensity I_{ASE} shows a superlinear increase versus ℓ for high J_p [Fig. 2(a)] which can be fitted with the usual equation:¹³ $I_{ASE}(\ell) = J_{sp}(\Omega) / g_{mod}(e^{g_{mod}\ell} - 1)$, where J_{sp} is the spontaneous emitted power corresponding to an appropriate emission solid angle Ω and g_{mod} is the small signal net modal optical gain. In Fig. 2(a), $g_{mod} = 12 \pm 3$ cm⁻¹.
- (iii) I_{ASE} shows a threshold behavior versus J_p [Fig. 2(b)]: at low J_p , $I_{ASE} \propto J_p^n$ with $n=0.5$ suggesting a strong Auger limited regime,¹⁷ while, for higher J_p , when the population inversion is achieved, $n \approx 3$ is measured, suggesting the onset of the stimulated emission regime.
- (iv) The lifetime of the fast component signal decreases significantly when the stimulated emission regime is entered [Fig. 2(b)]. From a rate equation analysis,^{8,12} a stimulated emission lifetime τ_{se} can be defined as

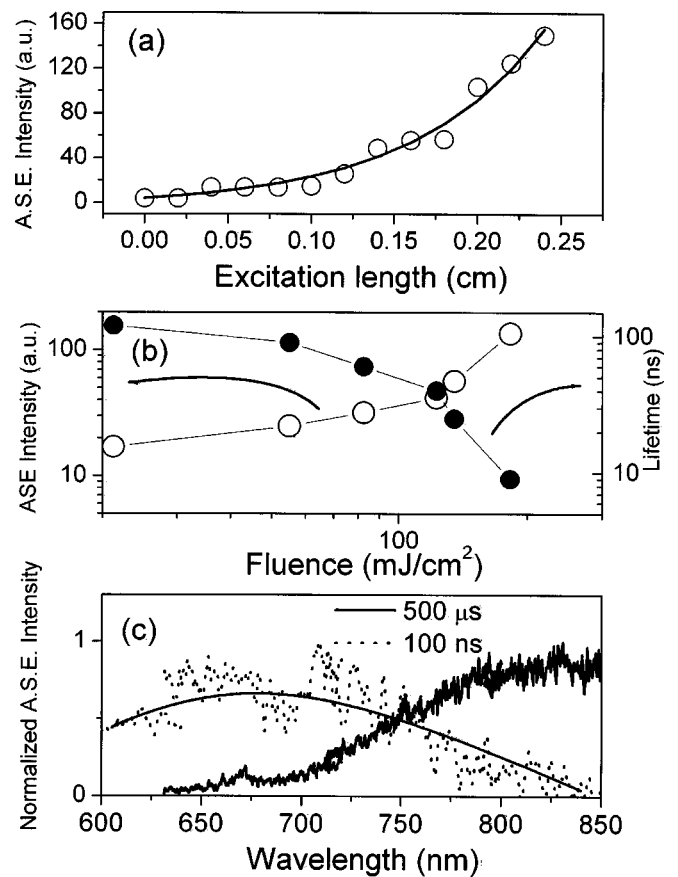


FIG. 2. (panel a) Points: ASE peak intensity at 760 nm vs the excitation length at pump fluence of 200 mJ/cm². Full line: Fit of the data with the one-dimensional amplifier model which yields a net modal gain value of 12 ± 3 cm⁻¹. (panel b) Open circles: ASE peak intensity of the fast component vs the pumping fluence. Filled circles: Lifetime of the ASE decay as a function of the pumping fluence. The lifetime has been extracted from the experimental decays as the $1/e$ intensity time. The solid lines are power-law fits to the intensity data. Excitation length was 2 mm. (panel c) ASE spectra measured for a fixed excitation length $\ell=2$ mm and pumping fluence of 200 mJ/cm² for two different integration time windows. Dotted line is the signal integrated during the first 100 ns after the excitation while the full line is the signal integrated for 500 μ s. The wavelength region is fixed by the experimental setup.

$\tau_{se} = 4/3 \pi R_{nc}^3 / \xi \sigma c n_{ph}$, where R_{nc} is the average Si ncs radius, ξ is the Si ncs volume fraction, σ is the emission cross section per nc, and n_{ph} is the number of emitted photons. An effective Auger recombination time can also be defined as $\tau_A = 1/2C_A N$, where C_A is an effective Auger coefficient and N is the density of photoexcited electron-hole pairs.¹² The initial slow decrease of the effective lifetime is probably due to the decrease of the Auger lifetime, while the fast decrease of the lifetime over the threshold is due to the fast decrease of the stimulated lifetime caused by the large increase of the amplified photon flux density (superlinear increase of I_{ASE}).

- (v) The fast component spectrum is broad and strongly blueshifted with respect to that of the slow component [Fig. 2(c)].

Let us comment in more detail on some of these characteristics. Our data demonstrate the presence of a fast recombination dynamics related both to the pumping intensity and to the pumped length. A fast component in the luminescence

decay of heavily photoexcited porous silicon has been attributed to Auger recombinations.^{17,18} Auger recombinations are indeed able to explain the appearance of a fast nonradiative recombination at high pumping rates (τ_A decreases as N increases, i.e., as J_p is increased), but they are always coupled with a saturation of the luminescence. On the contrary, we measured that I_{ASE} increases superlinearly both when the photon flux (proportional to n_{ph}) is increased by increasing ℓ [Fig. 2(a)] at a fixed J_p , and when, for long ℓ , J_p is increased. In addition, the Auger lifetime is independent on the internal photon flux while we measured a significant shortening of the lifetime (the fast component emerges from the slow component in the decay) when the excitation length is increased [Fig. 1(b)].

Edge emission intensity (I_{ASE}) turns out to be superlinear with respect to the pumping fluence above a characteristic threshold. This soft ASE threshold is a direct consequence of the onset of stimulated emission. The saturation exponent $n=0.5$ of the below threshold emission is typical of intranocrystals Auger recombination.^{17,18} The threshold separates two regimes (Auger and stimulated emission) where two different recombination mechanisms are present: either two very different recombination centers in the same Si-nc (i.e., defect centers and quantum confined excitons) or two different emission centers (e.g., two nc populations or defects in the SiO₂ matrix pumped through the Si-nc and exciton recombination in the Si-nc). One is dominating at low excitation powers and suffers of Auger saturation; while above a certain power threshold, the stimulated emission of the other is observed: These other centers are responsible for the observed optical gain. The presence of different recombination mechanisms in our sample is also evidenced by the clear difference in the spectral dependence of the fast and of the slow component. The strong blueshift in the fast component can be thought of as originating only from the gain-active centers that contribute above threshold. This scheme is compatible with a four-level model for the observed optical gain.^{2,12}

It is interesting to speculate about the nature of these centers. Defects in bare SiO₂ are excluded as bare SiO₂ does not show any optical gain at these wavelengths. Excess Si in SiO₂, possibly in the form of a Si-nc, is needed to observe optical gain. X-ray absorption studies and *ab initio* density functional theory calculations suggest that Si-nc in SiO₂ are coated by a 1 nm thick stressed silica shell.¹⁹ This stressed SiO₂ could enhance the formation of oxygen-related states, like silanone bonds,^{9,10,19–24} at the interface between a Si-nc and SiO₂ or in the stressed SiO₂ shell. The energy of a silanone-like bond as a function of the Si=O interatomic distances is typical of a four-level scheme, originating a significant Stokes shift between absorption and luminescence.^{10,20–23} Within this scheme, photon excitation induces a strong structural relaxation of small O-saturated nanocrystals leading to transitions involving surface localized states.²⁴ The broad and blueshifted gain spectrum could be understood in terms of molecularlike inhomogeneous

broadening mechanisms, such as different atomic surface configurations or strain fields, acting on small interface localized atoms or small silicon inclusions efficiently pumped by Si-nc through energy transfer.

In conclusion, optical gain dynamics have been studied in Si-nc samples. High-power time-resolved VSL measurements show the onset of stimulated emission with a fast inversion lifetime. The existence of two different recombination mechanisms within a four-level model for the optical gain was considered. It is clear that more theoretical and experimental works are needed to explain the observed fast gain in Si-nc.

This work has been supported by INFM through the project RAMSES. The authors acknowledge Z. Gaburro for technical support and fruitful discussion.

¹P. Ball, *Nature (London)* **409**, 974 (2001).

²*Towards the First Silicon Laser*, NATO Science Series, edited by L. Pavesi, S. Gaponenko, and L. Dal Negro (Kluwer, Dordrecht, 2003).

³L. Pavesi, L. Dal Negro, C. Mazzoleni, G. Franzò, and F. Priolo, *Nature (London)* **408**, 440 (2000).

⁴L. Khriachtchev, M. Rasanen, S. Novikov, and J. Sinkkonen, *Appl. Phys. Lett.* **79**, 1249 (2001).

⁵M. Nayfeh, S. Rao, N. Barry, A. Smith, and S. Chaieb, *Appl. Phys. Lett.* **80**, 121 (2002).

⁶K. Luterova, I. Pelant, I. Mikulskas, R. Tomasiunas, D. Muller, J. J. Grob, J. L. Rehspringer, and B. Hönerlage, *J. Appl. Phys.* **91**, 2896 (2002).

⁷A. V. Malko, A. A. Mikhailovsky, M. A. Petruska, J. A. Hollingsworth, H. Htoon, M. G. Bawendi, and V. I. Klimov, *Appl. Phys. Lett.* **81**, 1303 (2002).

⁸V. I. Klimov, A. A. Mikhailovsky, S. Xu, A. Malko, J. A. Hollingsworth, C. A. Leatherdale, H. J. Eisler, and M. G. Bawendi, *Science* **290**, 314 (2000).

⁹M. V. Wolkin, J. Jorne, P. M. Fauchet, G. Allan, and C. Delerue, *Phys. Rev. Lett.* **82**, 197 (1999).

¹⁰A. B. Filonov, S. Ossicini, F. Bassani, and F. Arnaud d'Avitaya, *Phys. Rev. B* **65**, 195317 (2002).

¹¹F. Iacona, G. Franzò, and C. Spinella, *J. Appl. Phys.* **87**, 1295 (2000); G. Vijaya Prakash, N. Daldosso, E. Degoli, F. Iacona, M. Cazzanelli, Z. Gaburro, G. Pucker, G. Dalba, F. Rocca, E. Ceretta-Moreira, G. Franzò, D. Pacifici, F. Priolo, C. Arcangeli, A. B. Filonov, S. Ossicini, and L. Pavesi, *J. Nanosci. Nanotechnol.* **1**, 159 (2001).

¹²L. Dal Negro, M. Cazzanelli, N. Daldosso, Z. Gaburro, L. Pavesi, F. Priolo, D. Pacifici, G. Franzò, and F. Iacona, *Physica E (Amsterdam)* **16**, 297 (2003).

¹³K. L. Shaklee, R. E. Nahaory, and R. F. Leheny, *J. Lumin.* **7**, 284 (1973).

¹⁴J. Valenta, I. Pelant, and J. Linnros, *Appl. Phys. Lett.* **81**, 1396 (2002).

¹⁵L. Dal Negro, P. Bettotti, Z. Gaburro, M. Cazzanelli, L. Pavesi, and D. Pacifici (unpublished).

¹⁶J. Linnros, A. Galeckas, N. Lalic, and V. Grivickas, *Thin Solid Films* **297**, 167 (1997).

¹⁷C. Delerue, M. Lannoo, and G. Allan, *Phys. Rev. Lett.* **75**, 2228 (1995).

¹⁸R. M'ghaieth, H. Maaref, I. Mihalcescu, and J. C. Vial, *Phys. Rev. B* **60**, 4450 (1999).

¹⁹N. Daldosso, G. Dalba, R. Grisenti, F. Rocca, L. Pavesi, F. Priolo, G. Franzò, and F. Iacona, *Physica E (Amsterdam)* **16**, 321 (2003); M. Luppi and S. Ossicini, *Phys. Status Solidi A* **197**, 251 (2003).

²⁰M. Caldas, *Phys. Status Solidi B* **217**, 641 (2000).

²¹A. Puzder, A. J. Williamson, J. C. Grossman, and G. Galli, *Phys. Rev. Lett.* **88**, 097401 (2002).

²²F. Zhou and J. D. Head, *J. Phys. Chem. B* **104**, 9981 (2000).

²³R. J. Baierle, M. J. Caldas, E. Molinari, and S. Ossicini, *Solid State Commun.* **102**, 545 (1997).

²⁴L. Khriachtchev, S. Novikov, and J. Lahtinen, *J. Appl. Phys.* **92**, 5856 (2002).